PAPER

Effect of Cr^{3+} on growth, thermal, photoluminescence and electrical properties of potassium dihydrogen citrate single crystal

Materials Research Express

PAPER

Effect of Cr^{3+} on growth, thermal, photoluminescence and electrical properties of potassium dihydrogen citrate single crystal

N D Pandya[1], J H Joshi[1], M J Joshi[1], D K Kanchan[2], Y H Gandhi[3] and H O Jethva[1]

[1] Department of Physics, Saurashtra University, Rajkot-360005 India
[2] Department of Physics, M.S. University of Baroda, Vadodara-390002 India
[3] Department of Applied Physics, Faculty of Engineering & Technology, M.S. University of Baroda, Vadodara-390002 India

E-mail: jaydeep_joshi1989@yahoo.com

RECEIVED
30 December 2018

REVISED
4 March 2019

ACCEPTED FOR PUBLICATION
22 May 2019

PUBLISHED
31 May 2019

Keywords: potassium dihydrogen citrate, powder XRD, TGA, photoluminescence, dielectric study

Abstract

Potassium Dihydrogen Citrate (KDC) is well recognized food additive and hence it is interesting to investigate the influence of toxic metal doping on its properties. The pure and 0.2 mol% Cr^{3+} doped KDC crystals are grown using solvent evaporation technique at room temperature. The grown crystals exhibits needle shape morphology. The EDAX analysis confirms the presence of chromium along with the constituent elements of KDC crystal. The powder XRD indicates the triclinic symmetry of the grown crystals. The FT-IR spectroscopic study indicates the presence of various functional groups in the pure and doped crystals. The Cr^{3+} improves the thermal stability of KDC crystal. The influence of Cr^{3+} doping is clearly shown by large value of dielectric constant of doped KDC crystals compared to pure KDC. The variation of dielectric constant, dielectric loss and A.C. conductivity with frequency are studied. The Photoluminescence study confirms the defect in hydrogen bonding network of KDC crystal due to doping of Cr^{3+}.

1. Introduction

Potassium Dihydrogen Citrate (KDC) is present in citrus fruits, kiwi, strawberries and many other fruits [1]. As a food additive, it finds several important roles in food and beverages [2]. It is also useful for performing various biological functions in human body such as to regulate the blood balance and acid-base balance in the blood and tissues [3]. KDC also exhibits great importance in the medical field as a medical aid of urolithiasis [4–7].

However, it is expected to study the defect formation due to Cr^{3+} by virtue of dielectric and PL studies. Previously, the Cr^{3+} doping is found to produce large impact on luminescence and fluroscence properties of variety of materials [8–10]. The toxicological and the carcinogeic impacts of Chromium is also well reported [11, 12]. Hence, it is more important to observe the effect of toxic metal doping on parent food additive compound.

Previously, few reports are published by different authors on pure and doped KDC crystals. For a instant, Love and Patterson [13], Zacharias and Glusker [14] and Van Auken [15] have reported crystal structure and solubility of citrate salt and double citrate salt. At a same time, certain reports are published on structural, micro-structural, thermal [16], optical and magnetic properties of VO^{2+} [17–19], Cu^{2+} [18] doped KDC crystals.

Moreover, none of the above mentioned authors have tempted to study the influence of metal ions on structural defect chemistry of KDC crystal. Hence, the present authors have chosen trivalent chromiam as dopant in KDC crystal and investigate its influence on certain physio chemical properties such as structural, spectroscopic, thermal, luminescent and dielectrical by mean of defect oriented approch.

2. Experimental technique

The growth of pure and 0.2 mol% Cr^{3+} doped KDC crystals are carried out using slow solvent evaporation technique at room temperature. The 100 ml saturated solution is prepared by adding KDC gravimetrically in

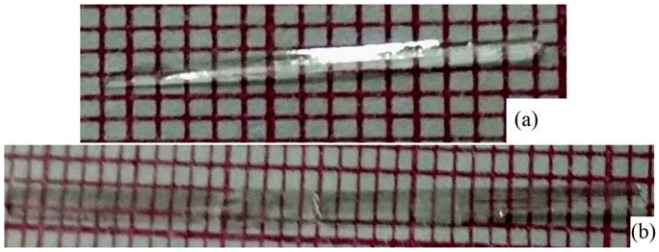

Figure 1. (a) Grown Pure KDC single crystal. (b) Grown 0.2 mol% Cr^{+3} doped KDC crystal.

double distilled water and then solution is stirred for 6 h to make the solution homogeneous. For the growth of Cr^{3+} doped KDC crystals, 0.0532 gm of chromium chloride hexahydrate ($CrCl_36H_2O$) is added and then the solution is again stirred for another 6 h. After the span of 12 h, both of the solutions are filtered and tranferred in glass vessels and shielded with porous lids to allow slow and controlled evaporation. The evaporation of solvent yielded crystallization of broad needle shaped, transparent and colorless pure KDC crystals, which are harvested after 20–25 days.

The Cr^{3+} doped KDC crystals are also found to be needle shaped, transparent and colorless. The photograph of grown pure KDC crystal is shown in the figure 1(a) and Cr^{3+} doped KDC crystal is shown in figure 1(b).

2.1. Characterization

The Powder XRD is carried out using PANaytical X'pert pro set up using CuK_α radiation within the range of 2θ values from 10° to 50° in steps of 0.02° sec^{-1} and the data are analysed using Powder X software. In the present study, the EDAX is performed on FEG Nano Nova SEM 450 instrument with resolution of 2 nm at 30 KV with W filament 3.5 nm at 30 KV. The FTIR study is carried out on the THERMO NIKOLET 6700 within the frequency range 4000 cm^{-1} to 400 cm^{-1} in KBr medium. TGA is carried out on the Linseis STA-PT-1600 from room temperature to 900 °C at heating rate 15° min^{-1} in an air atmosphere. The dielectric study is carried out using the pressed pellets of the samples of known dimensions at room temperature within the frequency 10 Hz to 10 MHz by using SOLARTRON SI 1260 Impedance/Gain-Phase Analyzer set up. The silver paste is used for proper electrical connection. The powdered samples are pelletized using die of 1 cm diameter by applying 2 tone pressure. The photoluminescence emission and absorption spectra are recorded at room temperature using Shimadzu RF-5301 PC spectro- fluoro- photometer and the Xenon is used as excitation source.

3. Results and discussion

3.1. Powder XRD

The figure 2 shows the powder XRD pattern of Cr^{+3} doped KDC crystal, which is compared with our earlier study of pure KDC crystal [20]. One can see that almost the same phase is observed on doping Cr^{+3} in KDC, however, there is a change in the peak intensity and minor shifts in peak positions. For example, the intensity of Cr^{+3} doped KDC sample peaks situated at 18.245°, 19.105°, 20.708°, 21.932°, 27.515° and 31.179° are changed in comparison to pure KDC; whereas the shifting in peak positions of Cr^{+3} doped KDC sample is found for peaks situated at 18.245°, 19.105°, 20.708°, 21.932°, 27.515°, 30.014° and 31.179° with comparison to pure KDC. From the above study, it is found that the peaks are shifted towards lower 2θ values for Cr^{+3} doped KDC.

Previously, the lattice parameters and unit cell volume of pure KDC crystals are found to be: a = 11.820 Å, b = 14.970 Å, c = 9.442 Å with angles $\alpha = 91.60°$, $\beta = 93.35°$, $\gamma = 110°$ and unit cell volume V = 1565.25 $Å^3$ [20]. In the present study, the lattice parameters and cell volume of Cr^{+3} doped KDC crystals are found to be: a = 11.840 Å, b = 14.940 Å, c = 9.442 Å with angles $\alpha = 91.52°$, $\beta = 93.35°$, $\gamma = 109.63°$ and unit cell volume V = 1568.57 $Å^3$. Both pure and doped KDC The grown crystals belong to triclinic system with space group P/1. The slight change in the lattice parameters, peak intensities and peak positions indicate the presence of dopant Cr^{+3}. The Cr^{3+} doped KDC crystal has exhibited single phase nature with no additional peaks observed. The peak shifting towards lower 2θ is due to planar tilting produced by compressive lattice strain produced by Cr^{3+} doping due to smaller ionic radius of Cr^{3+} ion (62 pm) with respect to K^+ ion (138 pm) [21].

3.2. Williamson-hall analysis

The dopant i.e. Cr^{3+} induces the lattice strain. The Williamson and Hall method is adopted to study the lattice strain in KDC crystal due to doping.

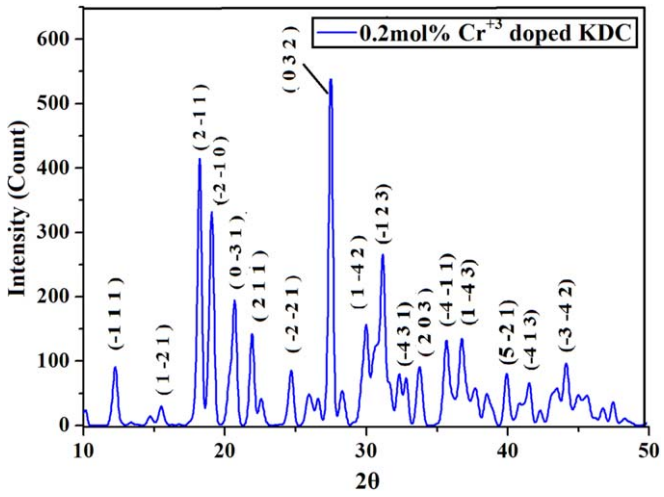

Figure 2. Powder XRD pattern of Cr^{+3} doped KDC.

Numerically, the Williamson and Hall equation is expressed below,[22]:

$$\beta_{hkl}\cos\theta = \frac{K\lambda}{D} + 4\varepsilon\sin\theta \quad (1)$$

where β_{hkl} is the Full Width Half Maximum (FWHM) of high internsity diffraction peaks, D is the Crystallite size, ε is the lattice strain, k is the 0.9 and λ is the source wave length is the 1.541 78 Å.

The value of the lattice strain for pure and Cr^{3+} doped KDC crystals is 0.067 and 0.076, respectively. Hence, the obtained values of lattice strain clearly indicates that the dopant causes defect in structure of KDC. Previously, the doping of bivalent and trivalent ions in KDP crystals is discussed in detail by Eremina *et al* [23].

When we are looking forward to the structural point of view of KDC crystal, the following argument can be proposed. The incorporation of Cr^{3+} ions in the KDC structure is expected to remove two potassium atoms and one proton according to geometric and valence balance requirements resulting in breaking of hydrogen bonds. The simultaneous breaking of hydrogen bonds and formation of two vacancies in the potassium positions introduces considerable changes in the chemical composition and substantial deformation of the nearest environment of the dopant ion but also introduces distortions. Thus the Cr^{+3} doping increases the lattice strain of KDC.

3.3. EDAX analysis

The EDAX spectrum is given in figure 3. The obatained weight percentage and atomic percentage is tabulated in table 1.

Here we have converted the atomic percentage to mole percentage to calculate the stiochiometry. The calculated mole percentages is tabulated in table 2.

The proposed and estimated stoichiometric formula are given in table 3. The proposed formula is based on the molar concentration of salt solution chromium (III) chloride hexahydrate added in KDC and the estimated formula obtained on the basis of EDAX results. The Cr^{3+} enters in less amount than expected from the molar concentration. This can be explained on the basis of large difference in the ionic radii of K^{+} (138 pm) and Cr^{3+} (62 pm). The smaller ionic radii leads to larger hydrated radii and the larger ionic radii gives smaller hydrated radii. Further, the larger hydrated radii leads to poor participation in forming compound as discussed earlier by Jethva *et al* [24]. It is also observed that the formation of hydrated radii depends on the electrostatic attraction between the ion and water molecules. The charge density of ion plays vital role in the electrostatic attraction between the charged ion and water molecules. Hence, considerable contribution of 3 + valency of Cr^{3+} is observed for the formation of hydrated radii. The non-hydrated radius of K^{+1} ion corresponding to first ionization potential 4.341 eV is 1.38 Å. Beside to K^{+1} the non-hydrated ionic radius of Cr^{+3} corresponding to third ionization potential 30.96 eV is found to be 0.52 Å. Hence the smaller concentration of Cr^{3+} ion is the consequence of large hydrated radius [25]. Thus, the estimated amount of chromium presence is lesser than potassium.

According to the Goldschmidt rule, the dopant ion can easily enter into the sites of parent crystal lattice if the difference of ionic radius between the doped ion and replaced ion does not increase more than 15%–20%, otherwise partial substitution of ions takes place [26]. In the present study, large difference is observed between

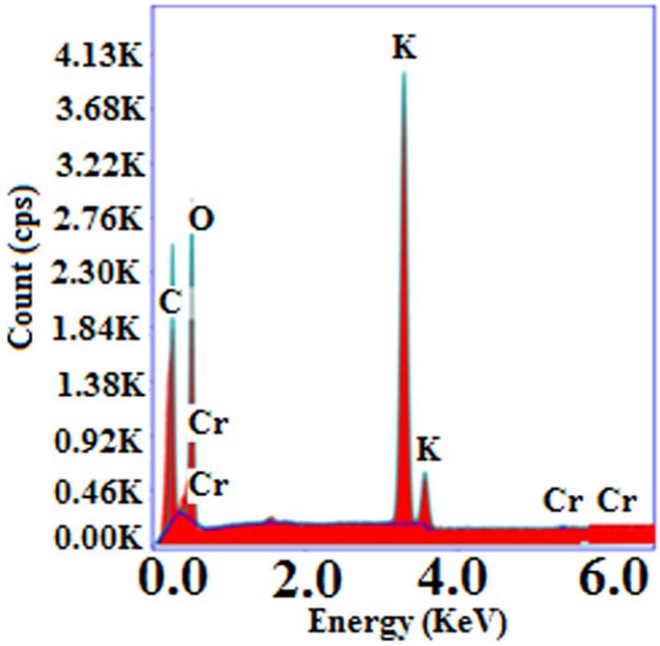

Figure 3. 0.2 mol% Cr^{+3} doped KDC EDAX spectrum.

Table 1. EDAX parameters of Cr^{3+} doped KDC.

Elements	Weight%	Atomic%
C (Carbon)	14.33	21.76
O (Oxygen)	56.87	64.84
K (Potassium)	28.51	13.30
Cr (Chromium)	0.28	0.10

Table 2. Elemental analysis of Cr^{+3} doped KDC crystal.

Element	Expected mole%	Observed mole%
K^{+1}	0.80	0.99
Cr^{+3}	0.20	0.01

Table 3. Proposed and estimated stoichiometric formula of Cr^{+3} doped KDC.

Proposed stoichiometric formula	Estimated stoichiometric formula
$C_6H_7K_{0.80}Cr_{0.2}O_7.nH_2O$	$C_6H_7K_{0.99}Cr_{0.01}O_7.nH_2O$

ionic radius of K^+ (138 pm) and Cr^{3+} (62 pm). As a result, small amount of Cr^{3+} doping takes place in the pure KDC.

3.4. FT-IR spectroscopic study

The FTIR study of KDC is reported by Marcilla *et al* [16] and also the FT-IR study of sodium citrate is reported by Laxmanan [27].

There are three hydrogen bond donors and seven hydrogen bond acceptors. It is expected that trivalent chromium doping may break one hydrogen bond and form two potassium vacancies. Due to this the doping of chromium in KDC is expected to bring some changes in vibrational behaviors of different functional groups and hence exhibit variations in the absorption peaks.

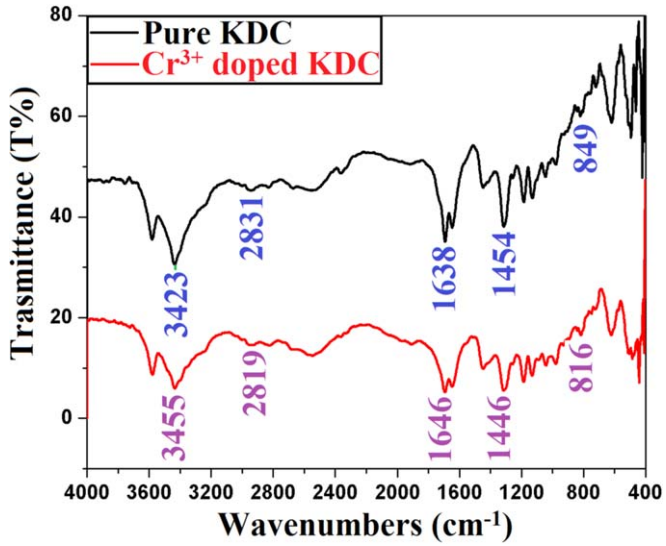

Figure 4. FTIR spectrum of KDC crystals. Potassium dihydrogen citrate (KDC) or potassium, 2- (carboxymethyl)—2,4 –dihydroxy—4—oxobutanoate ($C_6H_7KO_7$) possesses the following molecular structure. The figure 5 shows molecular structure of KDC crystal.

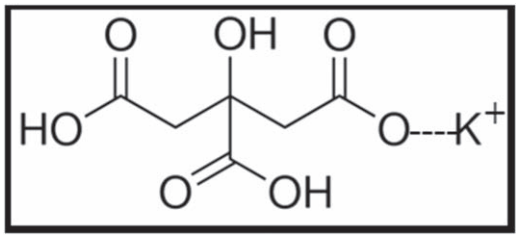

Figure 5. Molecular structure of potassium Di hydrogen citrate.

Table 4. FT-IR bond assignment of Cr^{3+} doped KDC.

Wave number (cm^{-1})		
Pure KDC [20]	Cr^{3+}doped KDC	Bond assignment
3423	3435	O–H stretching
2831	2819	CH_2 out of phase and in phase stretching vibrations
1638	1646	(symmetric and anti-symmetric) vibrations of O=C–OH carboxylate ion
1454	1446	
849	816	Metal-oxygen vibrations

In the present study the FTIR spectrum of figure 4 is compared with the FTIR spectrum of pure KDC. Table 4 gives the details of assignments of FTIR spectrum.

The frequency of the stretching vibration depends on: (1) the mass of the atoms and (2) the stiffness of the bonds. This has been reflected in FTIR spectra due to mass difference in potassium (atomic mass 39.08u) and chromium (atomic mass 51.9961u) atoms. The breaking of one hydrobgen bond is reflected in form of shifting in the frequency of vibrations involving hydrogen.

The relationship between the absorption frequency and the force constant is given by the following relation:

$$\nu = 1330\sqrt{F\left(\frac{1}{M_1} + \frac{1}{M_2}\right)} \tag{2}$$

where ν is the absorption frequency in (cm^{-1}), $1330 = (N_A \times 10)^{1/2}/2\pi c$,$M_1$ and M_2 are the atomic masses of the atoms (u). The force constants for pure and Cr^{3+} doped KDC are found to be 625 N m^{-1} and 632 N m^{-1} respectively.

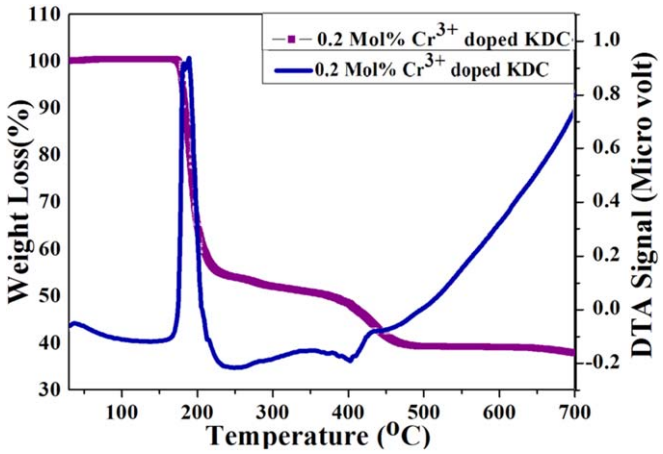

Figure 6. 0.2 mol% Cr^{+3} doped KDC TGA/DTA.

Table 5. Theoretical and experimental weight% of KDC.

T(°C)	Substance	Theoretical mass loss (%)	Experimental mass loss (%)
35 (R.T.)	$C_6H_7K_{0.99}Cr_{0.01}O_7.0.3H_2O$	100	100
175	$C_6H_7K_{0.99}Cr_{0.01}O_7$	99.76	99.76
213	$(K_{0.99}Cr_{0.01})_2CO_3$	59.95	57.81
500	$(K_{0.99}Cr_{0.01})_2O$	40.87	39.83

The Cr^{3+} doping in KDC is expected to create double occupied hydrogen bond (D-defect) with the hydrogen atom of O–H group, as a result the fundamental frequency of hydrogen gets altered.

Therefore, the present study clearly shows that, the force constant for O–H stretching vibrations is altered due to Cr^{3+} doping. The increase in force constant can also be correlated with the increase in lattice strain by considering linear proportionaliy between force and strain. Hence, for Cr^{3+} doped KDC, the increase in lattice strain corresponds to increase in force constant.

3.5. Thermal studies

The thermal study of KDC crystal is reported by Marcilla *et al* [16] by employing TGA on pure KDC and catalyst treated KDC.

The figure 6 shows TGA/DTA curves of 0.2mol% Cr^{3+} doped KDC crystal. Comparing the thermo-gram of pure KDC crystals [20], the Cr^{+3} doped KDC crystals exhibit a considerable difference. The pure KDC is dehydrated at 150 °C by giving up water molecules in two stages [20], but Cr^{+3} doped KDC exhibits thermal stability up to 175 °C without indication of loss of water molecules. This indicates that Cr^{+3} doped KDC is without appreciable amount of water of hydration or crystallization. At 213 °C, the carbonate stage occurs after precipitous decomposition at 175 °C. Further, at 500 °C the sample becomes oxide after the loss of carbon dioxide. Table 5 shows the theoretical and experimental weight loss in percentages at different temperatures using the stoichiometric formula obtained from EDAX data. The DTA study shows that only one exothermic peak is occurring at 175 °C indicating only one reaction into carbonate stage and removal of the moisture. The small endothermic reaction at 404 °C indicates the decomposition of carbonate into oxide by release of carbon dioxide.

It is important to note that the thermal stability of Cr^{3+} doped KDC is higher than pure KDC, which is not desirable because the chromium is toxic and its presence in KDC and ultimately in food products gives more thermal stability during cooking process and tends to remain in the product. This is unwanted effect of the chromium doping.

3.6. Photo-Luminiscence (PL) study

The photoluminiscence study of pure and Cr^{3+} doped KDC crystals are aimed to study the optical phenomena like recombination of the electron transitions at the specific wavelength taking place in the material. The figure 7 shows PL absorption spectra and the figures 8 and 9 shows the PL emission spectra of pure and Cr^{3+} doped KDC. The PL excitation wavelength is 254 nm and emission wavelength is 280 nm.

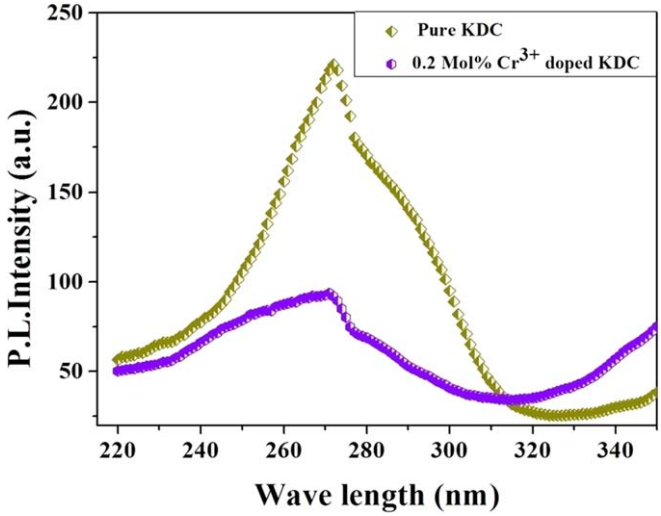

Figure 7. PL absorption spectra combined for pure and Cr^{3+} doped KDC.

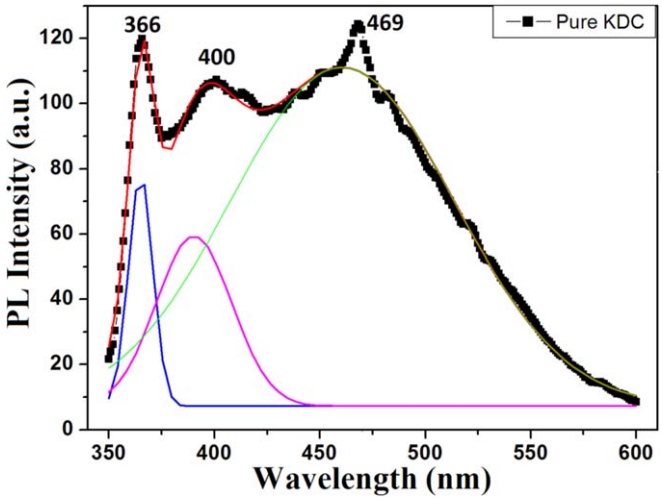

Figure 8. PL emission spectra of Pure KDC.

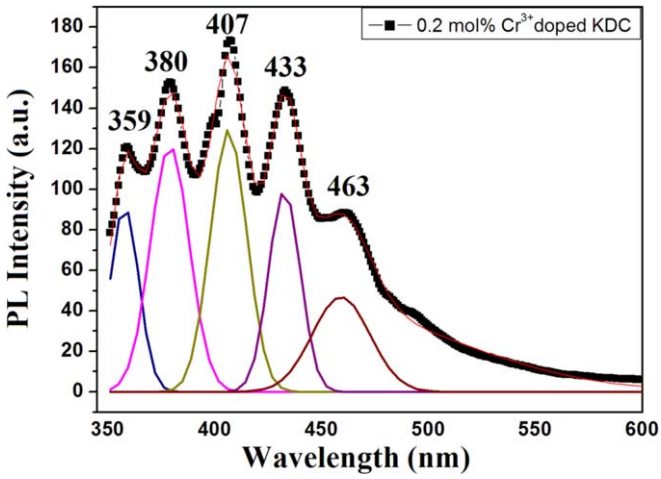

Figure 9. PL emission spectra of Cr^{3+} doped KDC.

Table 6. Gaussian fit analysis of pure and Cr^{3+} doped KDC.

Sr No	Type of crystal	UV emission (nm)	Violet emission (nm)	Blue emission (nm)
1.	Pure KDC	366, 400	—	469
2.	Cr^{3+} doped KDC	359, 380	407, 433	463

Table 7. PL Emission wavelengths for Pure and Cr^{3+} doped KDC.

Sample	Emission wavelength (nm)				
PURE KDC	—	366 (3.397 eV)	400 (3.10 eV)	469 (2.649 eV)	—
Cr^{3+} doped KDC	359 (blue shift) (3.463 eV)	380 (3.271 eV) (red shift)	407 (3.046 eV)	433 (2.863 eV) (blue shift)	463 (2.67 eV)
	L-defect (Unoccupied hydrogen bond)		D-defect (Double Occupied hydrogen bond)		

The given spectra exhibits mainly two emission peaks for pure KDC and four emission peaks for Cr^{3+} doped KDC crystal. The emission peak numbers are increases in the case of Cr^{3+} doped KDC crystals and the same are listed in table 5. The figures 8 and 9 show PL emission spectrum for pure KDC and Cr^{3+} doped KDC crystals, respectively, with Gaussian fitting to clearly identify the peaks. Table 6 gives the Gaussian fit analysis with different region emissions.

The PL emission spectra of Cr^{3+} doped KDC shows the additional peaks along with the considerable peak shifting. The emission spectra of pure KDC shows emission peaks at 366 nm (3.39 eV) corresponds to the unoccupied hydrogen bond (L-defect) and 469 nm (2.64 eV) corresponds to the double occupied hydrogen bond (D-defect). Now the addition of Cr^{3+} in KDC may able to break the hydrogen bonds from either central or terminal carboxyl group produces hydrogen vacancy (L-defect) to compensate with the charge neutrality.

Earlier, the presence of hydrogen vacancy due to deprotonation mode in sodium dihydrogen citrate compound is reported by Rammohan and Kaduk [28]. Similarly, in the present case, the mobile proton is generated due to L-defect in the lattice of KDC. Now the freely moving protons are further gets trapped by oxygen containing functional groups due to high electronegativity of the oxygen which is 3.44. Such combination produces the additional double occupied hydrogen bond (D-defect). The corresponding emission peaks and relative defect state is tabulated in table 7.

Here, from the given data in table 7 one can clearly find that the Cr^{3+} doping is able to break two additional hydrogen bonds to compensate the charge neutrality. As a result, the emission peaks positioned at 359 and 380 nm indicates the formation of hydrogen vacancy (L-defect). The trapping of these two freely moving protons by oxygen containing functional group creates double occupied hydrogen bond (D-defect). As a result, the formation of D-defect is shown by the emission peaks located at 407 and 433 nm.

The formation of D-defect is due to the lone pair of electrons contained by oxygen in oxygen containing functional groups. Each of these oxygens contains two lone pair of electrons tending to attract free protons generated due to L-defect. As the D-defect hinders the motion of the free protons, it gives rise to the reduction in the conductivity.

From the systematic study of potentiometric titrations, the libration of free protons due to incorporation of Cr^{3+} ions in lattice of citric acid to compensate the charge neutrality is reported by Hamanda *et al* [29].

Usually, the peak intensity of PL emission spectra is high for the material having comparatively less electrical conductivity [30]. As a result, Cr^{3+} doping reduces the conductivity of the pure KDC and hence the PL emission spectra of Cr^{3+} doped KDC shows high intensity emission peaks.

The high intensity of PL emission is the consequence of active optical properties of Cr^{3+} ions present in the host lattice of KDC. The presence of active electron in Cr^{3+} (electron configuration [Ar] $3d^3$) is related to $3d^3$ electrons. The energy levels of these active electrons undergo energy level splitting due to electron-electron interaction and crystal field effect by giving rise to change in intensity of PL emission spectra [31]. The degeneration of energy levels into $^4A_{2g}$, $^4T_{2g}$ and $^4T_{1g}$ states from the free Cr^{3+} ion $3d^3$ ground configuration is represented by Tanabe-Sugano diagram [32].

The PL absorption spectra of pure and Cr^{3+} doped KDC is shown in the figure 8. The wavelength difference for a same electronic transition between the position of band maxima of absorption and emission specra is defined as stokes shift [33]. The energy difference between emission and absorption band maxima is taken into account to find Stoke's shift for pure and Cr^{3+} doped KDC. The Stoke's shift difference for pure and Cr^{3+} doped KDC is given in table 8.

From the given results, it is confirmed that Cr^{3+} doping reduces the Stoke's shift. The existance of Stoke's shift is the outcome of vibrational energy relaxation phenomenon [34]. In the given context, the shifting of the

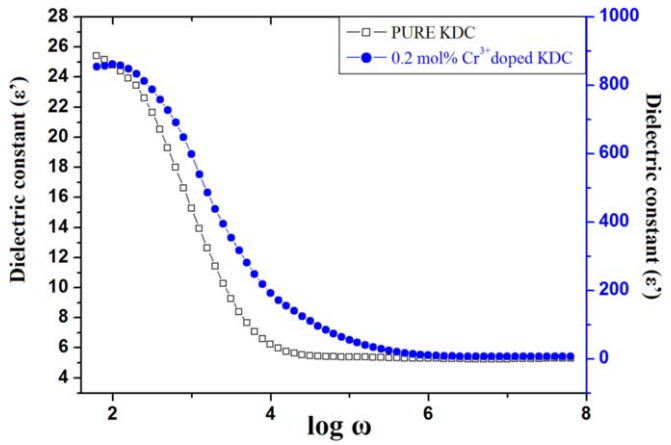

Figure 10. Pure and Cr^{3+} doped KDC dielectric constant combined.

Table 8. Variation in Stoke's shift of pure and Cr^{3+} doped KDC.

Sample	Absortion energy (eV)	Emission energy (eV)	Stoke's shift (eV)
Pure KDC	4.5 eV	2.64 eV	1.86 eV
Cr^{3+} doped KDC	4.5 eV	3.04 eV	1.43 eV

emission peaks towards lower wavelength takes place due to dissipation of energy followed by radiative emission [35]. As a result, considerable decrease in Stoke's shift takes place due to Cr^{3+} doping. The same results are obtained for the L-threonine doped ADP crystals [36].

3.7. Dielectric study

The complex impedance data of samples are taken into account to study dielectric properties. The dielectric contant (ε') and dielectric loss (tan δ) are calculated using the following equations:

$$\varepsilon' = \frac{t}{\omega A \varepsilon_0}\left[\frac{Z''}{Z'^2 + Z''^2}\right] \varepsilon'' = \left[\frac{Z'}{Z'^2 + Z''^2}\right] \tan\delta = \frac{\varepsilon''}{\varepsilon'} \quad (3)$$

where, A is the area of cross-section of the pellet, t is the thickness of the pellet, ε_o is the permittivity of the free space, Z′ is the real part of complex impedance, Z″ is the imaginary part of complex impedance. Further, ε' and ε'' are the real and imaginary part of complex permittivity.

3.7.1. Variation of dielectric constant (ε′)

The variation of dielectric constant as a function of the angular frequency for pure and Cr^{+3} doped KDC is given in figure 10. From the plots it is found that the dielectric constant retains the higher values for the lower frequencies. However, the increase in frequency of applied field leads to reduce the dielectric constant. The higher value of dielectric constant at lower frequency region is due to contributions of all the four polarizations, namely, electronic, ionic, and orientation and space charge polarizations [37]. From figures one can find that on doping Cr^{3+} in KDC increases the value of dielectric constant many times, viz, nearly 300 times in the low frequency region.

There are certain mechanisms proposed for this. Cunningham *et al* [38] have reported Cr^{+3} doping in ammonium dihydrogen phosphate (ADP) crystals. According to them the solution containing $CrCl_36H_2O$ on incorporation in ADP crystal lattice the cationic chromium complex $Cr_2Cl_2(H_2O)_4^+$ gives a compression of the bonding distance to the surrounding H_2O shell. As a result it replaces a single phosphate ion by a $Cr_2Cl_2(H_2O)_4^+$ complex. Further, the formal charge compensation is obtained through removal of two hydrogen bonding protons from the adjacent phosphate group and two adjacent ammonium cations. Moreover, Lai *et al* [39] have reported Cr^{+3} doping in potassium dihydrogen phosphate (KDP) crystals. They have suggested that the charge compensation is associated with impurity incorporation during growth is affected via hydrated impurity

complex displacing one bonding proton that binds two phosphate groups together with two potassium ions within the crystal structure to maintaining the charge balance.

The high dielectric constant value in the doped sample is due to charge compensation and vacancy produced in order to accomodate the trivalent chromium ion. This has been discussed in section 3.2 of present communication. The many fold higher values of dielectric constant of Cr^{3+} doped KDC crystals compared to pure KDC crystals in the low frequency region is thought to be very useful in terms of detection of toxic chromium in KDC after doing the necessary standardization process.

As the frequency of the applied field increases the dipoles cannot comply with the external field and hence the decrease in polarization gives rise to decrement in dielectric constant as the frequency increases. At higher frequency region the dielectric constants of both samples becomes constant as the polarization mechanism ceases to function when the applied field frequency becomes greater than relaxation frequency.

The dependence of dielectric constant on polarizibility can be explained by Clausius-Mosotti relation [40, 41].

$$\alpha = \frac{3M}{4\pi N_A \rho}\left[\frac{\varepsilon_\infty - 1}{\varepsilon_\infty + 1}\right] \tag{4}$$

where, α is the polarizibility, M is the molecular weight, N_A is the Avogadro number $= 6.022 \times 10^{23}$, ρ is the density and ε_∞ is the dielectric constant. The polarizibility of the pure KDC and Cr^{+3} doped KDC are found to be 42.38×10^{-23} cm^3 and 46.69×10^{-23} cm^3, respectively, at the frequency of 2 MHz and for the considered value of dielectric constants of 5.266 for pure and 7.054 for doped KDC crystals respectively. Here the polarizibility of Cr^{3+} doped KDC is slightly higher than pure KDC, however, the difference becomes rapidly larger at the lower frequency region.

As the polarizibility is related to the dielectric constant by the following relation:

$$\boldsymbol{\alpha} = \frac{\boldsymbol{\varepsilon_0}(\boldsymbol{K} - \mathbf{1})}{\boldsymbol{n}} \tag{5}$$

where, α = Strength of Polarizibility, K = Dielectric Constant, n = Number Density.

The above equation suggests that higher the value of dielectric constant, the higher is the polarizibility. The higher value of polarizibility of Cr^{3+} doped KDC as suggested in Jonscher's power law that leads the high value of dielectric constant of Cr^{3+} doped KDC crystal compare to pure KDC crystal.

Further, the reason for high dielectric constant of doped KDC crystal compare to pure KDC crystal can be interpreted as follows: since the variation in Stoke's shift is related to the vibrational relaxation phenomena in material and the dielectric constant is the measure of polarizibility, one can observed from the calculated Stoke's shift for pure and doped KDC crystals that, the Stoke's shift is reduced on doping the Cr^{3+} ion in KDC crystal that reflects the fact that the Cr^{3+} ion becomes polarized quickly compare to KDC and hence the resultant effect increases the polarizibility of Cr^{3+} doped KDC crystal (i.e. dielectric constant) compare to pure KDC crystal.

3.7.2. Variation of dielectric loss (D)

The dielectric loss (D) indicates the rate of dissipation of heat energy under the course electric field. The plots of dielectric loss (D) versus frequency for pure and Cr^{+3} doped KDC are given figure 11. The pure and Cr^{3+} doped KDC crystals display the dielectric loss behaviors in the same manner. Alike the nature of dielectric constant with angular frequency, the dielectric loss for doped sample is greater than pure KDC crystal, however, the magnitude of difference is very small. The doped sample exhibits higher dielectric loss compared to the pure sample indicating that the Cr^{+3} doping produces defect in the crystal. Moreover, as the Cr^{3+} doping promotes the D-defects in the lattice of KDC, it uses additional energy in terms of heat for the formation of double occupied hydrogen bond (D-defect) and as a result, the dielectric loss increases under the influence of Cr^{3+} doping [28].

3.7.3. Variation of A.C. conductivity

The a.c. conductivity is calculated by the following equation:

$$\boldsymbol{\sigma_{a.c.}} = \frac{\boldsymbol{z^{\backslash}}}{\boldsymbol{Z^{\backslash 2} + Z^{\backslash\backslash 2}}}\frac{\boldsymbol{t}}{\boldsymbol{A}} \tag{6}$$

where, Z′ and Z″ indicates the real and imaginary parts of impedance respectively, t is the thickness of the pellet and A is the area of the pellet.

Figure 12 shows the variation of a.c. conductivity with applied angular frequency for pure and Cr^{3+} doped KDC. From the above figure, it is found that conductivity of the material increases with increment in frequency of the applied field. The effect of Cr^{3+} doping is mainly observed in terms of diminished conductivity. Here, pure and doped KDC crystals exhibit almost constant value of a.c. conductivity at low frequency region which sharply jumps at the higher frequency.

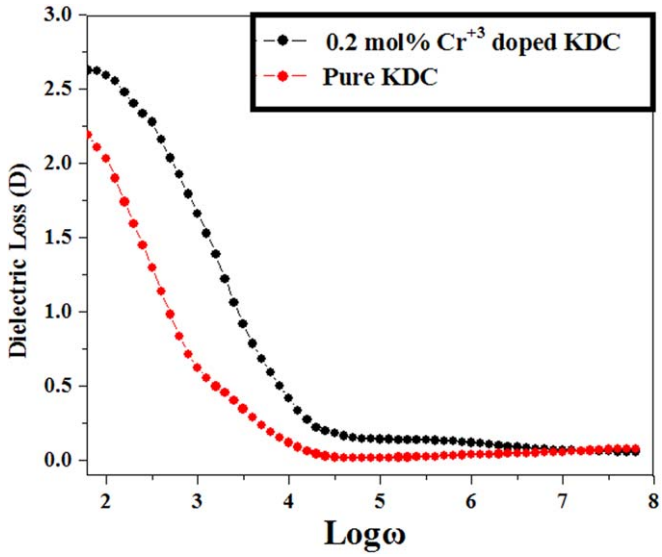

Figure 11. Dielectric loss pure and Cr^{+3} doped KDC combined.

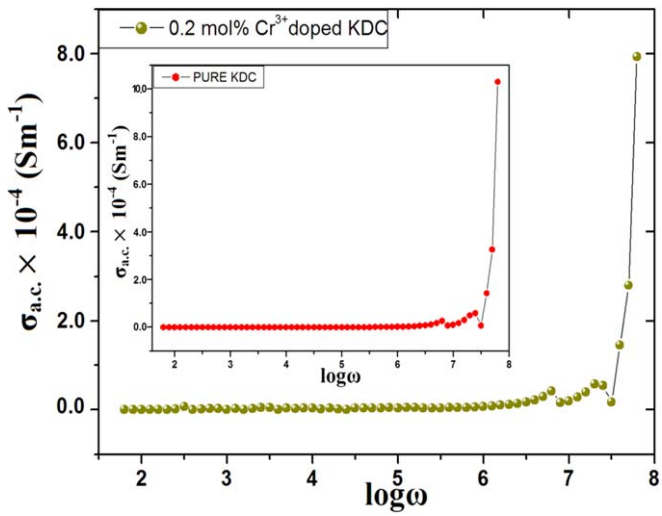

Figure 12. Plots of a.c. conductivity versus frequency for pure and Cr^{+3} doped KDC.

The conduction mechanism of pure and Cr^{3+} doped KDC can be explained by the deprotonation mode occurring in the material [28]. The incorporation of Cr^{3+} initiates the cationic charge imbalance occuring due to substitution of K^{+} ion by Cr^{3+}. The extra of 2 + valancy of Cr^{3+} gets compensated by breaking extra two hydrogen bonds from most likely from O–H containing functional groups. Subsequently, hydrogen vacancy is made called (L-defect). The protons released because of hydrogen vacancy further gets captured by oxygen containing functinal groups and produces double occupied hydrogen bond called (D-defect). Earlier, Joshi *et al* [42] have explained the details of protonic conduction in amino acid doped ADP crystals. In the Cr^{3+} doped KDC, the minor decrease in conductivity is due to the increase in D-defect. Joshi *et al* [43] already explained the role of D-defect in the decrease of conductivity.

3.7.4. Jonscher's plot

The Jonscher's power law can be expressed by the following equation [44]

$$\sigma_{\mathbf{total}} = \sigma_{\mathbf{d.c}} + \mathbf{A}\omega^{\mathbf{n}} \tag{7}$$

where, $\sigma_{d.c.}$ is termed as a frequency independent dc conductivity. However, the frequency dependent terms $A\omega^n$ represents the ac conductivity.

The dc conductivity is due to excitation of electron from localized energy state to conduction band. The term $A\omega^n$ is ac conductivity due to the dielectric dispersion phenomena, where n represents the degree of interaction

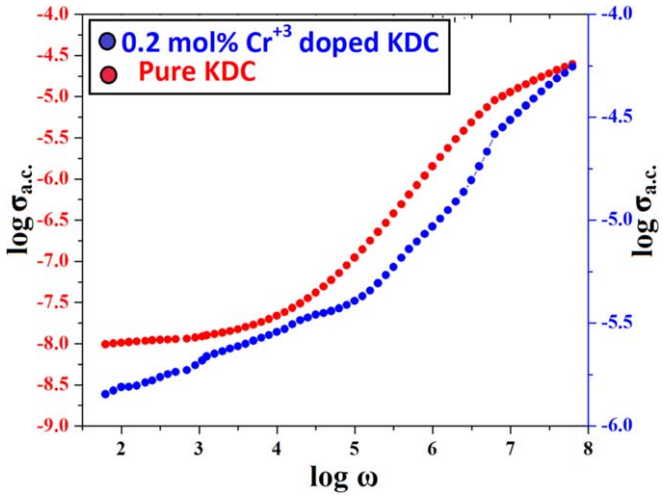

Figure 13. Pure & Cr^{+3} doped KDC Jonscher's plot combined.

Table 9. The Jonscher's plot parameters.

Sample	n	A ($S\,m^{-1}\,rad^{-n}$)	σ_{dc} ($S\,m^{-1}$)
$C_6H_7KO_7{\cdot}2H_2O$	0.16	4.46×10^{-9}	2.18×10^{-8}
$C_6H_7K_{0.988}Cr_{0.012}O_7{\cdot}0.3H_2O$	0.26	2.95×10^{-7}	—

between mobile ions with the lattice around them and A determines the strength of polarizibility. Figure 13 shows the Jonscher's plots of log σ_{ac} versus log ω. From the plots it is found that in the lower frequency region the conductivity almost remains constant for pure KDC crystals, while for the Cr^{+3} doped KDC crystals it displays highly dispersive nature for the same, indicating the absence of dc conductivity in the lower frequency region. In the lower frequency region $\sigma_{total}\,\alpha\,\sigma_{dc}$ for pure KDC, this shows the independence of conductivity with respect to the frequency of applied field. Further, in the higher frequency region $\sigma_{total}\,\alpha\,\omega^n$ is satisfied for all samples. The d.c. conductivity is diminished due to Cr^{+3} doping as shown in the figure 13. This may occur due to replacement of two K^+ ions and breaking of one hydrogen bond by Cr^{+3} ions. The simultaneous breaking of hydrogen bonds and formation of two vacancies in the potassium positions may facilitate the charge carriers motion leading to higher a.c. conductivity in the doped samples. Horlin and Bolt [45] have reported the influence of trivalent cation doping on ionic conductivity of KTP crystals.

From the Jonscher's plot of figure 10, the parameters A and n are calculated. The value of A is obtained from y-intercept and the value of n is obtained from the slope of the plots drawn. The calculated values of exponent n, constant A and σ_{dc} are represented in table 9.

From the above study it is observed that Cr^{+3} doping in KDC crystal increases the degree of interaction of mobile ions with the crystal lattice (n) and polarizibility strength (A). Further, this result gives confirmation to the increase in dielectric constant by Cr^{+3} doping.

The physical significance of degree of interaction of mobile ions with crystal lattice (n) is explained by Funke [46], viz., for $n \leqslant 1$ corresponding to hopping involving translational motion with a sudden hopping and $n > 1$ involving a small hopping without leaving neighborhood [47]. For ionic conductors the value of n ranges between 1 and 0.5 indicating ideal long range pathways and diffusion limited hopping (tortuous pathways) [48]. However, the Jump Relaxation Model (JRM) developed by Funke and Reiss [49] signifies the dispersion in the conductivity to strong forward–backward jump correlations in the motion of ions. In the present study $n < 1$ suggested the hopping involving translational motion with a sudden hopping.

4. Conclusion

The pure and Cr^{3+} doped KDC crystals are grown by slow-solvent evaporation technique. The grown Cr^{3+} doped KDC crystals displayed the triclinic symmetry and single phase nature with needle type morphology. The presence of chromium is identified by EDAX and the stoichiometric formula is proposed. The presence of various functional groups is confirmed by FTIR spectroscopy and slight shifting is observed in the absorption peaks responsible to O–H, CH_2, O=C–OH functional groups in comparision to pure KDC. From TGA it is

found that Cr^{+3} doped KDC possessed more thermal stability compared to pure KDC. The Cr^{+3} doping drastically increased the dielectric constant. The higher value of dielectric constant in Cr^{+3} doped KDC is due to charge balance compensation leading to higher polarization then in the pure KDC. Both the crystals obeyed Jonscher's power law and parameter A and n are evaluated. The value of $n < 1$ suggested the hopping of charge carriers involving translational motion with sudden hopping. The doping of Cr^{3+} introduces hydrogen bonding associated L-defects and D-defects to achieve charge compensation in KDC crystals. That is further supported by the PL studies and dielectric studies.

From the present study, one can draw two major conclusions: (1) the Cr^{+3} doped KDC is more thermally stable than pure KDC and (2) the Cr^{+3} doped KDC possess more dielectric constant than pure KDC. The higher thermal stability of toxic Cr^{+3} doped KDC is unwanted property in food aditives containing KDC because its thermal degradation does not take place readily at lower temperatures below 175 °C and higher possibility to remain in food products even temperatures higher or equal to boiling point of water. Comparatively very high dielectric constant values of Cr^{3+} doped KDC may be useful to detect the presence of toxic chromium in low concentration in food products by suitable application of dielectric spectroscopy study after proper standardization.

Acknowledgments

The authors are thankful to UGC, New Delhi, for funding under DRS-SAP and DST for funding under FIST. The authors are thankful to HOD, Physics, of Saurashtra University, Rajkot and HOD of Physics as well as Applied Physics Departments of M S University of Baroda, for their keen interest. One of the authors (JHJ) is highly thankful to Mr S G Khandelwal, Deputy Director, Forensic Science Laboratory, Ahmadabad for allowing him to carry out such research activity.

ORCID iDs

N D Pandya https://orcid.org/0000-0003-0731-9818

References

[1] Potassium dihydrogen citrate: IN 332(i) (www.foodnetindia.in)
[2] Sinclair C 1998 *Dictionary of Food* (USA: A & C Black Publishers Ltd)
[3] Hass E M Role of Potassium in Maintaining Health (www.hkpp.org/patients/potassium-health)
[4] Treatment with potassium citrate, Hypocitraturia (www.emedicine.medscape.com/article/444968-overview#a15)
[5] Caudarella R and Vescini F 2009 Urinary citrate and renal stone disease: the preventive role of alkali citrate treatment *Arch. Ital. Urol. Androl.* **81** 182
[6] Krieger N S, Asplin J R, Frick K K, Granja I, Culbertson C D, Ng A, Grynpas M D and Bushinsky D A 2015 Effect of potassium citrate on calcium phosphate stones in a model of hypercalciuria *J. Am. Soc. Nephrol.* **26** 3001
[7] Pak C Y C *Potassium Citrate Therapy of Nephrolithiasis* (Berlin: Springer) (https://doi.org/10.1007/978-1-4613-2069-2_8)
[8] Bodke M R, Gawai U P, Khawal H K and Dole B N 2015 131–33 Structural, photoluminescence and Raman spectroscopy studies on Cr substituted ZnS nanocrystals(ICFMM) 8(3)
[9] Salcedoa W J, Bragab M S and Jaimes F V V R 2018 Huge enhancement of photoluminiscence emission from porous silicon film doped with Cr (III) ions, Huge enhancement of photoluminiscence emission from porous silicon film doped with Cr(III) ions *J. Lumin.* **199** 109–11
[10] Luan T, Liu J, Yuan X and Li J 2017 Controlled hydrothermal synthesis and photoluminiscence of nanocrystalline $ZnGa_2O_4$: Cr^{3+} monospheres *Nano. Res. Lett.* **12** 219
[11] Hamada Y Z, Bayakly N, Peipho A and Carlson B Accurate potentiometeric studies of chromium-citrate and ferric-citrate complexes in aqueous solutions at physiological and alkaline pH values *Synthesis and Reactivity in Inorganic, Metal-Organic, and Nano-Metal Chemistry* **36** 469–76
[12] Sun H, Brocato J and Costa M 2015 Oral chromium exposure and toxicity *Curr. Environ. Health Rep.* **2** 1295
[13] Love W E and Patterson A L 1993 X-ray crystal analysis of the substrates of aconitase, III, crystallization, cell constants and space groups of some alkali citrates *Acta. Cryst.* **13** 426–8
[14] Zacharias D E and Glusker J P 1993 Structure of a citrate double salt: potassium di-hydrogen citrate–lithium potassium hydrogen citrate monohydrate *Acta. Cryst.* **C49** 1727–30
[15] Van Auken T V 1991 Solubility and heat of solution of potassium dihydrogen citrate *J. Chem. Eng. Data* **36** 255–7
[16] Marcilla A, Gomez A, Beltron M, Berenguer D, Martinez I and Blasco I 2017 TGA-FTIR study of the thermal and SBA-15-catalytic pyrolysis of potassium citrate under nitrogen and air atmospheres *J. Anal. & Appl. Pyrolysis.* **125** 144
[17] Aygun Z 2013 *J. Chem. Cryst.*AFM and SEM studies of VO^{2+} doped potassium dihydrogen citrate single crystal obtained by slow evaporation method **43** 103–7
[18] Aygun Z 2013 Variable temperature EPR studies of Cu^{2+} and VO^{2+} doped potassium dihydrogen citrate ($C_6H_7KO_7$) *Spectrochim. Acta* **104** 130–3
[19] Yarbaşi Z, Karabulut A and Karabulut B 2011 EPR and optical studies of vanadium doped potassium dihydrogen citrate ($C_6H_7KO_7$) single crystal *Spectrochim. Acta* **79** 1304–7
[20] Pandya N D, Joshi J H, Jethva H O and Joshi M J 2017 Structural, spectroscopic and thermal studies of potassium Di-hydrogen citrate crystal *Mech. Mater. Sci. Eng.* **10** 2412–595

[21] Cullity B D 1956 *Elements of X-ray Diffraction* (United States of America: Addition Wesley Publishing Company)
[22] Willamson G K and Hall W H 1953 X-ray line broadening from filed aluminium and wolframL'elargissement des raies de rayons x obtenues des limailles d'aluminium et de tungstene Die verbreiterung der roentgeninterferenzlinien von aluminium- und wolframspaenen *Acta Metall.* **1** 22–31
[23] Eremina T A, Eremin N N, Furmanova N G, Kuznetsov V A, Okhrimenko T M and Urusov V S 2001 Comparative characterization of defects formed by Di-and trivalent metal dopants in KDP crystals and the structural mechanism of influence of impurities on face morphology *Cryst. Rep.* **46** 82
[24] Jethva H O, Vyas P M, Tank K P and Joshi M J 2014 FTIR and thermal studies of gel-grown, lead–cadmium-mixed levotartrate crystals *J. Ther. Anal. Calor.* **10** 1388–6150
[25] Jethva H O, Kanchan D K and Joshi M J 2016 Impedance and dielectric studies of gel grown lead-iron mixed levo tartrate crystals *Int. J. Inter. Res. Sci. Eng. Tech.* **5** 2319–8753
[26] Murray T F and Dungan R H 1964 Oxygen firing can replace hot pressing for PZT *Cerem. Ind.* **82** 74
[27] Laxmanan B R 1964 Infra red apsorption spectrum of sodium citrate *J. Ind. Inst. Sci.* **38** 68
[28] Rammohan A and James A A 2016 Second polymorph of sodium dihydrogen citrate, $NaH_2C_6H_5O_7$: structure solution from powder diffraction data and DFT comparison, commeunications *Acta. Cryst.* E **72** 854–7
[29] Hamada Y Z, Carson B L and Shank J T 2003 Potentiometric and UV–vis spectroscopy studies of citrate with the hexaquo Fe^{3+} and Cr^{3+} metal ions *Synth. React. Inorg. Met.-Org. Chem.* **33** 1425–40
[30] Portia S A U, Jayanthi K and Ramamoorthy K 2014 Growth and characterization of pure and disodium hydrogen phosphate mixed with potassium dihydrogen phosphate crystal by using slow evaporation technique *Amr. J. Bio. Pharm. Res.* **1** 77–82
[31] Berusuker I B 1998 *Electronic Structures and Properties of Transition Metal Compounds* (United States of America: Wiley)
[32] Sugano S, Tanabe Y and Kamimura H 1970 *Multiplets of Transition-Metal Ions in Crystals* (New York: Acaemic)
[33] Gispert J R 2008 *Co-Ordination Chemistry* (United States of America: Wiley-VCH) pp 483
[34] Hiroshi F and Straub J E 2005 Vibrational energy relaxation in proteins *PNAS* **102** 6726–31
[35] Takmakoff A 2009 *Lecture Notes on Vibrational Relaxation* (United States of America: MIT Department of Chemistry)
[36] Joshi J H, Kalainathan S, Kanchan D K, Joshi M J and Parikh K D 2018 Effect of L-threonine on growth and properties of ammonium dihydrogen phosphate crystal *Arab. J.Chem.* (https://doi.org/10.1016/j.arabjc.2017.12.005)
[37] Parikh K D, Dave D J and Joshi M J 2009 Crystal growth, thermal, optical, and dielectric properties of L-lysine doped KDP crystals *Moder. Phys. Lett.* B **12** 1589–602
[38] Cunningham D A H, Hammond R B, Lai X and Roberts K J 1995 Understanding the habit modification of ammonium dihydrogen phosphate by chromium ions using a dopant-induced charge compensation model *Chem. Mater.* **7** 1690
[39] Lai X, Roberts K J, Bedzyk M J, Lyman P I, Cardoso L P and Sasaki J M 2005 Structure of habit modifying trivalent transition metal cations (Mn^{3+}, Cr^{3+} *Chem. Mater.* **17** 4054
[40] Joshi J H, Dixit K P, Joshi M J and Parikh K D 2016 Study on A.C. electrical properties of pure and L-serine doped ADP crystals *AIP Confer. Proceed.* **1728** 020219
[41] Haung J P and Yu K W 2007 *New Nonlinear Optial Materials: Theoretical Research* (New York: Nova Publication)
[42] Joshi J H, Dixit K P, Parikh K D, Jethva H O, Kanchan D K, Kalainathan S and Joshi M J 2018 Effect of Sr^{2+} on growth and properties of ammonium dihydrogen phosphate single crystal *Journal of Material Science:Materials in Electronics* **29** 5837–852
[43] Joshi J H., Kanchan D.K., Jethva H.O., Joshi M.J. and Parikh K.D. 2018 Dielectric relaxation, protonic defect, conductivity mechanisms, complex impedance and modulus spectroscopic studies of pure and L-threonine-doped ammonium dihydrogen phosphate *Ionics* **24** 1995–2016
[44] Jonscher A K 1977 The 'universal' dielectric response *Nature* **256** 673
[45] Horlin T and Bolt R 1995 Influence of trivalent cation doping on the ionic conductivity of $KTiOPO_4$ *Sol. Stat. Ion.* **78** 55
[46] Funke K 1993 Prog. Jump relaxation in solid electrolytes *Sol. Stat. Chem.* **22** 111
[47] Sen S and Chaudhary R N P 2004 Impedance studies of Sr modified $BaZr_{0.05}Ti_{0.95}O_3$ ceramics *Mater. Chem. Phys.* **87** 256
[48] Mauritz K A 1989 Dielectric relaxation studies of ion motions in electrolyte-containing perfluorosulfonate ionomers long-range ion transport *Macromole.* **22** 4483
[49] Funke K and Reiss I 1984 Debye—Huckel—Type relaxation processes in solid ionic conductors *Z. Phys. Chem. Neue Folge.* **140** 217